and shorten the effective ^{15}N T_1. Previous solid-state NMR studies on α-LP (*24*) indicated an optimal mixing time for CP of 0.3 ms for protonated nitrogens and 2 ms for nonprotonated nitrogens. Mixing times of 1.5 to 2 ms were used for the spectra reported here. The ^{15}N and ^{1}H frequencies were 32 and 318 MHz, respectively, and the ^{1}H 90° pulse length was 3.0 μs. The sample temperature was maintained near 170 K or 240 K with cooled N_2 as the spinning gas. The low temperature served to increase sensitivity and reduce dielectric heating of the sample.
15. To adjust the *p*H of the enzyme crystals for *p*H-dependent NMR studies, the crystals were separated from the mother liquor by mild centrifugation and resuspended in 0.6*M* Li_2SO_4 at the desired *p*H and incubated at room temperature for ∼15 min to allow for equilibration throughout the crystal. [The meaning of *p*H and pK_a in solid samples has been discussed (*24, 25*). The process was repeated until equilibration at the desired *p*H was attained. The *p*H of the mother liquor was measured on a Radiometer *p*H meter (model 260) with a combination electrode (model GK2322C) at 295 K. The titration was reversible, the direction of the titration did not affect the relative intensities of the NMR resonances. Also, the entire titration was repeated on the same crystals and spectra recorded at 240 K. Chemical shifts are relative to external 1*M* $H^{15}NO_3$ in ^2H_2O, with positive shifts being upfield, and referenced to the *p*H independent signal of the natural abundance ^{15}N amide backbone resonance at 255 ppm. No correction was made for bulk magnetic susceptibility effects which are expected to be small.
16. Intensity of the $^{15}N\delta 1$ signal as a function of *p*H was fit to the Henderson-Hasselbalch equation with the use of the program *Enzfitter—A Nonlinear Data Analysis Program for the IBM PC* [R. Leatherbarrow (Elsevier-Biosoft, Cambridge, 1987)].
17. Solution state ^{15}N NMR studies show that the addition of 0.6*M* Li_2SO_4 to a solution of α-LP in 0.1*M* KCl increases the pK_a of His^{57} from 7.0 to 7.5 (S. Farr-Jones and W. W. Bachovchin, unpublished data).
18. D. M. Blow, J. J. Birktoft, B. S. Hartley, *Nature* **221**, 337 (1969).
19. C. S. Craik, S. Roczniak, C. Largeman, W. J. Rutter, *Science* **237**, 909 (1987).
20. S. Sprang *et al.*, *ibid.*, p 905.
21. P. Carter and J. A. Wells, *Nature* **332**, 564 (1988).
22. W. W. Bachovchin and J. D. Roberts, *J. Am. Chem. Soc.* **100**, 8041 (1978).
23. M. N. G. James and L. B. Smillie, *Nature* **224**, 694 (1969).
24. T. H. Huang, W. W. Bachovchin, R. G. Griffin, C. M. Dobson, *Biochemistry* **23**, 5933 (1984).
25. M. Munowitz *et al.*, *J. Am. Chem. Soc.* **104**, 1192 (1982).
26. Supported by NIH research grants GM 27927 and GM 23403, a postdoctoral fellowship to S.O.S. (GM 10502), Research Career Development Award to W.W.B. (DK 01122), and NSF equipment grant PCM 8212656. The Stable Isotopes Resource of the Los Alamos National Laboratory provided $^{15}NH_3$ for the synthesis of the ^{15}N-labeled histidines with the aid of NIH grant RR 02231. We thank D. Agard for advice on crystallizing α-LP and helpful discussions.

12 December 1988; accepted 14 March 1989

Ice Core Evidence for Extensive Melting of the Greenland Ice Sheet in the Last Interglacial

R. M. Koerner

Evidence from ice at the bottom of ice cores from the Canadian Arctic Islands and Camp Century and Dye-3 in Greenland suggests that the Greenland ice sheet melted extensively or completely during the last interglacial period more than 100 ka (thousand years ago), in contrast to earlier interpretations. The presence of dirt particles in the basal ice has previously been thought to indicate that the base of the ice sheets had melted and that the evidence for the time of original growth of these ice masses had been destroyed. However, the particles most likely blew onto the ice when the dimensions of the ice caps and ice sheets were much smaller. Ice texture, gas content, and other evidence also suggest that the basal ice at each drill site is superimposed ice, a type of ice typical of the early growth stages of an ice cap or ice sheet. If the present-day ice masses began their growth during the last interglacial, the ice sheet from the earlier (Illinoian) glacial period must have competely or largely melted during the early part of the same interglacial period. If such melting did occur, the 6-meter higher-than-present sea level during the Sangamon cannot be attributed to disintegration of the West Antarctic ice sheet, as has been suggested.

INTERPRETATION OF THE AGE AND mode of origin of the ice sheets and ice caps has been difficult because drag and melting at the base of these ice sheets may have disturbed or removed the record in the deepest and oldest ice. Studies of oxygen isotopes (δ^{18}O) and pollen concentrations in a core from the top of the flow line on Agassiz ice cap, Ellesmere Island, Canada (Fig. 1), led to the conclusion that the lowermost 3 m of ice were deposited during the last (Sangamon) interglacial period (*1*). The location must, therefore, have been ice-free earlier during the same interglacial. Because of certain similarities among this core and others drilled from the same ice cap and on Devon ice cap, this interpretation was extended to include the Canadian Arctic Island (CAI) ice caps in general (Fig. 1) (*1*). A similar origin for the basal ice in the ice cores from Camp Century (CC) and Dye-3 (D3) (Fig. 1) has been cursorily suggested (*2, 3*), and a study of diatoms in the basal debris of the CC core showed that this drill site was ice-free during some interglacial in the past (*4*). In this report, I review the record from the Greenland and Antarctic cores to evaluate the possibility that the ice-free period at the CC and D3 drill sites was the last interglacial (*5*).

I use Core 79 from Agassiz ice cap (Fig. 2) as representative of all the CAI cores (Table 1) because it is from a drill site close to the top of the flow line and has been intensively studied (*1, 6–8*). Byrd and Vostok cores are from Antarctica; D3 and CC are located on the Greenland ice cap. Dating for all these cores has been achieved by various methods (*9–11*) but is largely speculative beyond 13 ka (*2, 12*). However, for assessing the age of the basal ice with respect to the last interglacial, a rough time scale is adequate.

There are three main sections in the δ^{18}O record of the CAI and Greenland cores (Fig. 1): (i) an uppermost one (A in Fig. 1) representing the present interglacial period (0 to 10 ka); (ii) a middle section (B) with more negative values representing the last glaciation (10 to 110 ka); and (iii) a lowermost section (C), where δ^{18}O values are less negative again. In general, negative δ^{18}O values represent cold climatic conditions and less negative values, warmer conditions. The δ^{18}O records, together with ice texture and cation, pollen, and microparticle concentrations (*1, 9, 13, 14*), indicate that the CAI cores include these three ice core sections even though the CAI ice caps are much thinner than the ice sheets of Greenland and Antarctica (Table I). The Vostok core, which does not reach bedrock, includes all these sections, spans the entire last interglacial period, and includes also part of the glacial period before that (*3*). The Byrd core covers the top two sections (*11*) and has been arguably considered to include Sangamon ice at its base (*15*).

Comparisons between the observed δ^{18}O values of the basal and mean Holocene ice in the CAI and Greenland ice cores suggest that the basal ice in all these cores was deposited during an interglacial climate (Table 2). However, correction of the Greenland ice core data is necessary to account for the effect of elevation on the basal δ^{18}O values (*17, 18*): because of the nature of glacier flow, the deepest ice forms from snow deposited on the surface well up the flow line, and δ^{18}O values become more negative with increasing elevation in Greenland (*16*). Correction of the CAI data is not necessary as, at present, elevation is not related to δ^{18}O values in the Canadian Arctic Islands (*19*), and the cores I am considering

---

Terrain Sciences Division, Geological Survey of Canada, Ottawa, Ontario K1A OE8.

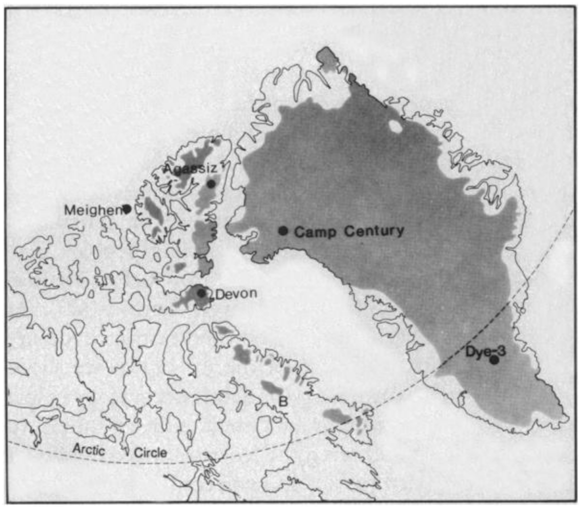

Fig. 1. Location map. The shaded areas represent ice-covered areas; B, Barnes ice cap.

are from close to or at the top of the flow line. The elevation-corrected basal $\delta^{18}O$ values from Greenland, including the values from the section with more negative $\delta^{18}O$ values 1.7 to 8 m above the bed in the CC core (Table 2, column 4), are all much less negative (warmer) than Holocene values. They indicate that the snow was deposited in an interglacial climate. However, the Greenland values are so "warm" that they are incompatible with a steady-state ice sheet but consistent with snow deposited at much lower elevations. Reeh (*20*) arrived at a similar conclusion for the CC core from a non–steady-state modeling approach. Consequently, it is appropriate to consider a limiting case where the snow (that is, the lower parts of section C in the D3 and CC cores) was deposited on bedrock during the initial stages of ice sheet growth. The bedrock was then at a higher elevation because it was without an ice load. To calculate a basal $\delta^{18}O$ value ($\delta^{18}O_{bed}$) representative of snow deposited at such an elevation during an interglacial period, the present mean Holocene $\delta^{18}O$ value at the Greenland sites ($\delta^{18}O_{obs}$) was adjusted to the lower elevation according to:

$$\delta^{18}O_{bed} = \delta^{18}O_{obs} + 0.006\ (0.66\ h)$$

where 0.006 is the $\delta^{18}O$ change (in per mil) per 1 m change of elevation, and 0.66 is an adjustment for the effect of isostatic uplift on the elevation of the bed. Because this ice originates at or close to the bed, it could not have traveled far since its deposition. To simplify matters, I assume that it was deposited at the present position of the drill site. Thus h is the present ice thickness there in meters (Table 1).

The calculated basal values (Table 2) are slightly warmer than the observed ones but sufficiently similar to lend support to the hypothesis that the basal ice formed from snow deposited on uplifted bedrock during the last interglacial. The section 1.7 to 8 m above the bed in the CC core has $\delta^{18}O_{bed}$ values "cold" enough to suggest that deposition took place on a thinner-than-present ice sheet, that is, at elevations higher than even the isostatically elevated bedrock. This ice would have been deposited as the ice thickness increased and would have come from up the flow line. Both factors suggest deposition of ice at higher elevations and thus more negative $\delta^{18}O$ values. In addition, I show below that the basal layers are probably formed of superimposed ice where the temperature-$\delta^{18}O$ relation is complicated by fractionation during the melting and refreezing cycle (*21*).

The basal ice of all the CAI cores (Table 1 and lower part of Fig. 1C) has a very low air bubble content; in the Devon ice cap cores it is 60% that of the bulk of the Holocene ice and 20% that of the glacial period ice (*13*). The lower part of the Holocene section in the Agassiz 79 and 84 cores also has a low bubble content. The texture of this Holocene ice indicates that it formed by the melting and refreezing of surface snow during a warm period of the early Holocene, about 7 to 9 ka. The bubble texture of both this and the low bubble content basal ice is similar to that of superimposed ice (*22*). Meighen ice cap consists almost entirely of superimposed ice (*23*), as does a large part of the Barnes ice cap (*24*) (Fig. 2).

The bottom 15.7 m of the CC core has a gas content of 51 ml per kilogram of ice, which is 50% less than that in the rest of the core (*25*). Similarly, the total gas concentration in the bottom 22 m of the D3 core is 64.7 to 65.3 ml per kilogram of ice, only 66% of that in the ice above it (*26*). In contrast, the debris-laden basal ice in the Byrd core, which will be shown below to have been formed by basal freeze-on processes, is almost devoid of gas bubbles (2 ml air per kilogram of ice) (*27*). An abrupt change to over 100 ml of air per kilogram of ice occurs at the boundary between this ice and the debris-free ice above (*27*). In support of the hypothesis that the basal layers of the CC core were formed by basal freeze-on, Herron and Langway have suggested that the gas inclusions there (51 ml per kilogram of ice) are the result of diffusion of gases from overlying ice during 10,000 years of pressure melting point conditions at the bed (*25*). However, the same process should have caused at least a slight diffusion of gas across the boundary between debris-laden and clean ice at Byrd, but did not. Perhaps a better explanation of the different bubble texture in the CC basal ice (and that of D3 also) from that of the bulk of the ice core overlying it is that the basal ice formed as superimposed ice.

Table 1. Ice core parameters.

Core	Surface temperature (°C)	Basal temperature (°C)	Ice thickness (m)	Surface accumulation rate (m/year)	Surface elevation (m)
		Agassiz ice cap			
A 77	−24.5	−16.7	338	0.175	1670
A 79	−22.3	−19.0	139	0.115	1700
A 84	−21.9	−19.1	127	0.100	1730
		Devon ice cap			
D 72 and D 73	−23.1	−18.4	299	0.220	1800
		Meighen ice cap			
M 65	−17.5	−15.9	121	0.095	260
		Greenland ice cap			
Camp Century (CC)	−24.4	−13.0	1388	0.380	1885
Dye-3 (D3)	−18.0	−13.2	2037	0.550	2485
		Antarctica			
Vostok	−55.5	*	3700	0.024	3488
Byrd	−28.0	−1.6	2164	0.130	1515

*Data not available.

The high CO_2 content of the basal ice at CC (*25*) and D3 (*26*) provide further support for this interpretation. Melting of snow and its subsequent refreezing (when at the surface and not as ice at the base of an ice sheet) has been associated with high CO_2 content (*26*). Stauffer *et al.* (*26*) (with reference to the D3 core) "could not exclude the possibility that the ice from the silty layer was temperate at the time of formation." The high CO_2 concentrations in the CC basal ice have been attributed to oxidation of methane (*25*). A simpler explanation is that the ice formed as superimposed ice; superimposed ice layers in the upper (A in Fig. 2) sections of D3 have similar high CO_2 concentrations (*26*).

If basal melt has occurred at any of the core sites since the deposition of the ice now at the bottom of the various ice sheets, then the ice representing the initial growth of the ice sheets will be lost: it will either have run off beneath the ice sheet or refrozen elsewhere at a location remote from the drill site location. The presence of basal debris in the lowermost layers of all the cores has been cited as evidence that melt or freeze-on had occurred in the past (*8, 15, 25, 28*).

The basal layers of the Agassiz ice cap cores (A 79, A 84), which are from the top of the flow line, and the two deep Greenland cores (Table 1 and Fig. 2) contain visible dirt particles and rare pebble-sized material (*7, 8, 25, 28*). The A 77 and Devon ice cap cores include basal ice with a few dirt clots composed of silt-sized material (*13, 14*). The lowermost 15.7 m of the CC core contain over 300 layers of clear and debris-laden ice (*25*). The particles range in size from 2 to 200 μm; one 20-mm-long pebble was found. The average debris content in the debris-laden zone is 0.24% by weight (*25*). The debris in the basal ice of the D3 core has not been studied in detail but it appears to be similar in grain size and concentration to that in the CC core (*29*).

The dirt particles have been considered to be too large to have been wind-borne (*25, 28*), presumably because the paleo ice cap in each case is believed to have been of similar proportions to the present one. Instead, it has been argued that debris inclusion was by freeze-on at the bed. However, the basal inclusions in the CAI and Greenland cores are markedly different from the debris composing the marginal moraines in both Greenland (*30*) and Devon ice caps. These moraines form at the edges of ice caps and ice sheets as a result of melting out and deposition of material carried in the ice. They were the subject of the original freeze-on hypothesis (*31*). The moraines include material that is much larger than that in the cores.

A large size fraction also characterizes the basal debris in the Byrd core where the basal ice is at the pressure melting point and water is found at the bed-ice interface, indicating that the debris was most likely incorporated by freeze-on (*27*). Yet there is a large difference between the concentration and size of material in the CAI, CC, and D3 cores on the one hand and the Byrd core on the other. The Byrd core contains cobble-sized material and the debris concentration is about 12 to 15%, by weight, more than 50 times that measured in the CC and CAI cores.

The freeze-on explanation for debris inclusion in the CAI and Greenland cores is questionable on other grounds also: (i) The sub-ice material is evidently porous at two of the CAI drill sites (*32*). Freeze-on at the bed should result in an impermeable layer under the ice cap. (ii) Production of a sequence of melt and freeze-on at the bed requires a subtle balance between surface snow accumulation rates, surface temperature, and ice thickness. However, these conditions vary greatly between the Greenland and CAI core sites (Table 1 and Fig. 2). The dissimilarities make it most unlikely that melt or freeze-on mechanisms, even for 100,000 years, could produce basal ice at each of these sites with common signatures in terms of relatively low air bubble content, debris inclusions covering similar size ranges, and interglacial isotope signatures. (iii) Marine diatoms are abundant in the unconsolidated sediments under the CC drill site but there are only freshwater diatoms in the ice above (*4*). Freeze-on should have incorporated the marine diatoms from the subglacial sediments in the basal layers (unless marine diatoms are absent from the subglacial sediments upstream).

Alternatively the debris now in the CAI and Greenland basal ice could have been incorporated during the initial stages of ice growth in the cooler parts of the last interglacial period, more than 100 ka. During its initial growth, an ice sheet develops from a snowfield where melting is not quite sufficient to remove the previous winter snow. Growth is almost certainly in the form of superimposed ice that will have a variable but typically low bubble content but will rarely be bubble-free (*23*). At this stage of growth, ice-free areas are common and these areas will provide a source of material of various size ranges, including pebbles. Several small ice caps may grow before coalescing into fewer and larger ice caps (*33*). As the ice-free areas become restricted in size with expansion of the ice cap or ice sheet, the source areas for debris become fewer and more distant. Consequently, windblown dust will reach the ice cap surface in smaller concentrations and will consist of finer particles. Such a gradation is evident in the CC basal ice where the sand-sized fraction decreases and the silt-sized fraction increases with height above the bed (*25*). Similarly, dirt layers in a 121-m surface-to-bedrock core from the top of Meighen ice cap, which has been stagnant throughout its 4000-year history, decrease in number up from the bed to the surface (*23*). As the ice cap or ice sheet thickens and expands, its increasing surface elevation results in cooler summer conditions with or without a climatic cooling trend. The bubble percentage in the ice will increase as the percentage of firn increases.

Apart from the Meighen ice cap, buried dirt layers have been found in other stagnant bodies of ice less than 4000 years old. For example, a small 8-m-thick ice field on Melville Island (Northwest Territories, Canada) has appreciable amounts of pebble-sized sediment more than 1 m above its bed (*34*). This ice cap is stagnant, generally less than 40 m thick, and composed of superimposed ice. Dirt layers are also common in the ice at the base of permanent snowbanks (*35*). In all of these cases debris incorporation into the ice occurred either at the same time as, or not long after, that ice formed.

If freeze-on can be discounted, the possibility of loss of the oldest ice in the CAI and Greenland cores by melting also becomes

Table 2. Observed and calculated basal $\delta^{18}O$ values in per mil. Column 5 shows basal values corrected for a higher elevation of deposition up the flow line. The elevation increase is 1000 m for CC [figure 5.3 in (*17*)] and 346 m for D3 [figures 1 and 5 in (*18*)]. Column 6 shows values from column 3 corrected for deposition on uplifted bedrock at the present drill sites (see text).

Core site	Ice thickness (m)	Observed $\delta^{18}O$		Calculated basal $\delta^{18}O$	
		Holocene	Base	Elevation corrected	Uplifted bed
Dye-3	2037	−27.9	−23.2	−21.0	−19.8
Camp Century	1388	−29.0	−25.0 (−30.5)*	−18.6 (−26.1)*	−23.5
Agassiz 79	139	−26.7	−25.1	−25.1	†

*Section with very negative $\delta^{18}O$ values 1.7 to 8.0 m above the bed. †Not applicable, as there is no elevation effect at this site.

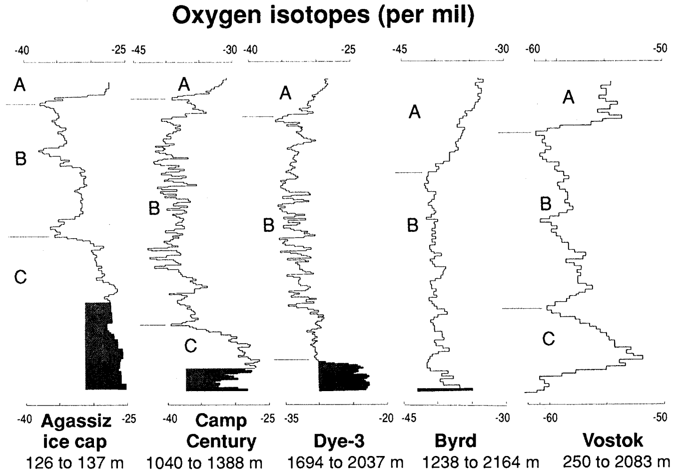

Fig. 2. Oxygen isotope ($\delta^{18}O$) profiles. The Agassiz ice cap profile is A 79 (Table 1). The $\delta^{18}O$ scale is expanded for the Vostok profile. Note that the vertical depth scales differ substantially from profile to profile. Each is plotted on a linear depth scale with different resolutions; the depth section plotted is shown under the title heading for each site. Each profile with the exception of that for Vostok has the bed-ice interface at the bottom of the diagram. The shaded zones are where visible dirt inclusions occur. A, Holocene ice; B, main part of the last glacial period; C, glacial-interglacial transition and Sangamon ice. The evidence for an interglacial origin for the basal ice at Byrd station is questionable (*15*), as it could as well be glacial period ice with older ice than this having melted at the base (see text).

questionable. A study of the temperatures in the D3 borehole (*36*) concluded that the basal temperature in the D3 borehole has never risen above −12°C for 115,000 years (*37*).

I suggest that the basal layers in the CAI and Greenland surface-to-bedrock ice cores are of interglacial (Sangamon) age and that the ice dates the onset of glaciation at, and up the flow line from, the drill sites. Because the CAI cores are from the highest points of two of the larger ice caps in the islands, glacier retreat may have been complete there at that time. In Greenland, retreat must have been at least as far back as the present positions of the two drill sites. The implication from D3 is that the southern dome completely melted. The main drainage channel, which begins under the highest part of the ice sheet (approximately 71°N, 36°W) and ends at Jakobshavns Isfjord (*38*), may have divided the Greenland ice sheet into two parts during the retreat process, especially if massive drawdown during a retreat cycle occurred (*39*). Such retreat may mean that the oldest ice, if there is any that predates the last interglacial period, lies to the north of the present, highest part of the ice sheet.

Massive (and possible complete) retreat of the Greenland ice sheet would account for a large part (or all) of the 6-m rise in sea level that occurred during the last interglacial period. Therefore, the West Antarctic ice sheet could not have surged at that time as loss of the West Antarctic ice sheet and all, or a great part of, the Greenland ice sheet would have caused a sea-level rise greatly in excess of values derived from coral reef studies (*40*). Recent oceanographic data (*41*) also suggest that the West Antarctic ice sheet was stable. Boreholes either through the Greenland ice sheet at its thickest and highest parts or in the central part of Greenland to the northwest of this would help determine the extent of the Greenland ice sheet during the last interglacial period.

The CAI ice caps and Greenland ice sheet may have melted more extensively in the last interglacial period than in the present one because of higher insolation maxima at that time (*42*). Ice core evidence shows that maximum melting of the Agassiz ice cap during the present interglacial period, 8 to 9 ka, occurred close to the peak of insolation maximum at 10 ka; melting and insolation values have both gradually decreased since then. However, the timing of the last interglacial period and its relation to orbital forcing is disputed (*43*). What appears to be needed is a greatly improved time scale for the various paleoclimate indicators.

REFERENCES AND NOTES

1. R. M. Koerner, J. C. Bourgeois, D. A. Fisher, *Ann. Glaciol.* **10**, 85 (1988).
2. W. Dansgaard *et al.*, *Science* **218**, 1273 (1982).
3. C. Lorius *et al.*, *Nature* **316**, 6029 (1985).
4. D. M. Harwood, *Arctic* **39**, 4 (1986).
5. The term "interglacial" is imprecise when used with reference to the last interglacial as it may apply to Ocean stage 5e alone or may span the entire Ocean stage 5. The problem is discussed at length in D. St Onge, *Geogr. Phys. Quat.* **41**, 2 (1987).
6. D. A. Fisher *et al.*, *Nature* **301**, 5897 (1983).
7. R. M. Koerner, D. A. Fisher, M. Parnandi, *Ann. Glaciol.* **2**, 34 (1981).
8. R. M. Koerner, D. A. Fisher, W. S. B. Paterson, *Can. J. Earth Sci.* **24**, 296 (1987).
9. W. S. B. Paterson *et al.*, *Nature* **266**, 5602 (1977).
10. C. U. Hammer *et al.*, *J. Glaciol.* **20**, 82 (1978).
11. S. J. Johnsen, W. Dansgaard, H. B. Clausen, C. C. Langway, Jr., *Nature* **235**, 434 (1972).
12. W. Dansgaard, H. B. Clausen, N. Gundestrup, S. J. Johnsen, C. Rygner, in *Greenland Ice Core: Geophysics, Geochemistry and the Environment*, C. C. Langway, Jr., H. Oeschger, W. Dansgaard, Eds. (Monograph 33, American Geophysical Union, Washington, DC, 1985), pp. 77–84.
13. R. M. Koerner and D. A. Fisher, *J. Glaciol.* **23**, 89 (1979).
14. D. A. Fisher and R. M. Koerner, *ibid.* **32**, 122 (1986).
15. G. Boulton and U. Spring, *ibid.*, p. 112.
16. W. Dansgaard, S. J. Johnsen, H. B. Clausen, N. Gundestrup, *Medd. Gronl.* **197**, 2 (1973).
17. W. F. Budd and N. W. Young, in *The Climatic Record in Polar Ice Sheets*, G. deQ Robin, Ed. (Cambridge Univ. Press, Cambridge, 1983), pp. 150–177.
18. N. Reeh, S. J. Johnsen, D. Dahl-Jensen, in *Greenland Ice Core: Geophysics, Geochemistry and the Environment*, C. C. Langway, H. Oeschger, W. Dansgaard, Eds. (Monograph 33, American Geophysical Union, Washington, DC, 1985), pp. 57–65.
19. R. M. Koerner, *J. Glaciol.* **2**, 86 (1979).
20. N. Reeh, Proceedings of a workshop on the Geological History of the Polar Oceans: Arctic versus Antarctic, 10 to 14 October 1988, Bremen (in press).
21. R. M. Koerner, W. S. B. Paterson, H. R. Krouse, *Nature Phys. Sci.* **245**, 148 (1973).
22. Superimposed ice forms when surface snow melts and percolates to the ice surface underneath to refreeze. In warm summers, some of the annual snow layer leaves the ice cap as run-off; low bubble content ice is left behind to form an attenuated annual layer. Cooler summers are associated with less run-off and bubble-rich ice. Continued summer cooling leads to decreased melt and, eventually, accumulation in the form of firn. Compression of firn under accumulating layers of snow and firn above it results in common glacier ice. Because run-off comes from part of the annual layer, it leaves a mean annual $\delta^{18}O$ value unrepresentative of the prevailing precipitation temperature (*21*). This form of ice is fully discussed in R. M. Koerner, *Geogr. Ann.* **52A**, 1 (1970).
23. R. M. Koerner, *J. Glaciol.* **7**, 51 (1968).
24. R. LeB. Hooke, *ibid.* **17**, 75 (1976).
25. S. Herron and C. C. Langway, Jr., *ibid.* **23**, 89 (1979).
26. B. Stauffer, A. Neftel, H. Oeschger, J. Schwander, in *Greenland Ice Core: Geophysics, Geochemistry and the Environment*, C. C. Langway, H. Oeschger, W. Dansgaard, Eds. (Monograph 33, American Geophysical Union, Washington, DC, 1985), pp. 85–89.
27. A. J. Gow, S. Epstein, W. Sheehy, *J. Glaciol.* **23**, 89 (1979).
28. A. M. D. Gemmell, M. J. Sharp, D. E. Sugden, *Earch Sci. Proc. Landf.* **11**, 123.
29. C. U. Hammer *et al.*, in *Greenland Ice Core: Geophysics, Geochemistry and the Environment*, C. C. Langway, H. Oeschger, W. Dansgaard, Eds. (Monograph 33, American Geophysical Union, Washington, DC, 1985), pp. 90–94.
30. B. L. Bishop, *U.S. Army Cold Reg. Res. Eng. Lab. Res. Rep. 17* (1958).
31. J. Weertman, *J. Glaciol.* **3**, 30 (1961).
32. Diesel oil was used to fill the Agassiz ice cap 1977 drill hole (1 km downslope of core 79) to a height of 260 m above the bed, which is the firn/ice transition level. One day later the level of oil had dropped to 50 m above the bed. It is assumed that the excess diesel oil had drained through the bed. Similarly, 50 liters of water that had been melted from the bottom of hole 87 (1 km up the summit ridge from core 79) drained away through the bed. In both cases there was no evidence in the cores that there were cracks in the ice at a depth that allowed the liquids to drain away from the hole.
33. R. F. Flint, *Glacial and Quaternary Geology* (Wiley, New York, 1971). This is slightly different from Flint's concept of small mountain glaciers coalescing into piedmont glaciers and moving on to lower lying land to form the main body of the ice sheet.
34. D. Harry, personal communication.
35. G. Ostrem, *Geogr. Ann.* **45**, 4 (1963).
36. D. Dahl-Jensen and S. J. Johnsen, *Nature* **320**, 6059 (1986).
37. In the non-steady-state model (*34*) it is assumed that the ice thickness remains constant but that surface temperature and precipitation rates vary. However, a model beginning with a zero ice thickness more than 100 ka would yield lower basal temperatures because the thickness in the early stage of ice cap growth is decreased.
38. A. Weidick, Compiler, *Quaternary Map of Greenland* (Geological Survey of Greenland).

39. T. Hughes, in *North America and Adjacent Oceans During the Last Deglaciation*, W. F. Ruddiman and H. E. Wright, Jr., Eds., vol. K3 of *Geology of North America*, (Geological Society of America, Boulder, 1987), pp. 183–220.
40. J. Chappell and N. J. Shackleton, *Nature* **324**, 137 (1986).
41. P. F. Barker *et al.*, *ibid.* **328**, 6126 (1987).
42. Well referenced and described in R. S. Bradley, *Quaternary Paleoclimatology* (Allen and Unwin, Boston, 1985).
43. I. J. Winograd, B. J. Szabo, T. B. Coplen, A. C. Riggs, *Science* **242**, 4883 (1988).
44. I thank the Geophysical Isotope Laboratory of the University of Copenhagen for access to data concerning the Greenland cores. D. A. Fisher also gave considerable help in reviewing early drafts of the manuscript and organized the transfer of some of the raw core data. The concept of massive melting of the Greenland ice sheet arose from frequent discussions with both D. A. Fisher and N. Reeh. Work on this paper began when the author was working with the Polar Continental Shelf Project of Energy Mines and Resources. This paper is contribution no. 35888 of the Geological Survey of Canada.

3 November 1988; accepted 11 April 1989

Membranes as the Energy Source in the Endergonic Transformation of Vitamin A to 11-*cis*-Retinol

PETER S. DEIGNER, WING C. LAW, FRANCISCO J. CAÑADA, ROBERT R. RANDO*

The eye needs to biosynthesize 11-*cis*-retinoids because the chromophore of rhodopsin is 11-*cis*-retinal. The critical metabolic step is the endergonic isomerization of free all-*trans*-retinol (vitamin A) into 11-*cis*-retinol. This isomerization process can take place in isolated membranes from the retinal pigment epithelium in the absence of added energy sources. Specific binding proteins probably do not serve as an energy source, and since all of the reactions in the visual cycle are shown here to be reversible, trapping reactions also do not participate in the isomerization reaction. One previously unexplored possibility is that the chemical energy in the bonds of the membrane itself may drive the isomerization reaction. A group transfer reaction is proposed that forms a retinyl ester from a lipid acyl donor and vitamin A. This transfer can drive the isomerization reaction because the all-*trans*-retinyl ester is isomerized directly to 11-*cis*-retinol. Thus, the free energy of hydrolysis of the ester is coupled to the thermodynamically uphill trans to cis isomerization. The prediction of an obligate C–O bond cleavage in the vitamin A moiety during isomerization is borne out. Although the natural substrate for isomerization is not known, all-*trans*-retinyl palmitate is processed in vitro to 11-*cis*-retinol by pigment epithelial membranes.

THE ISOMERIZATION OF FREE ALL-*trans*-retinol (vitamin A) into 11-*cis*-retinol in the retinal pigment epithelium provides the visual chromophore and closes the visual cycle. In the absence of this process vertebrate vision would be impossible, because 11-*cis*-retinoids are produced only in the eyes of image-forming animals and are not dietary constituents. The 11-*cis*-retinoids are approximately 4 kcal/mol higher in free energy than their all-*trans* congeners, and thus account for only 0.1% of the equilibrium mixture (*1*). Yet in an animal adapted to darkness, 11-*cis*-retinoids can account for ~75% of the retinoids (*2*). Hence, an energy-requiring step seems to be necessary.

A membrane fraction from the retinal pigment epithelium has been isolated that can process exogenous all-*trans*-retinol to 11-*cis*-retinol, 11-*cis*-retinal, and 11-*cis*-retinyl esters (*3*). The process is saturable with a Michaelis constant (K_m) of 0.5 μM and a basal maximal velocity (V_{max}) of 5 pmol $hour^{-1}$ mg^{-1} of protein, and 11-*cis*-retinoids accumulate to account for up to 40% of the total retinoids (*4*). The conversion occurs in the absence of added energy sources such as adenosine 5′-triphosphate, guanosine 5′-triphosphate, and palmitoyl coenzyme A. Likewise, the addition of these agents does not stimulate 11-*cis*-retinoid production, suggesting that soluble cofactors are not required for the isomerization (*4*) and that the energy source is membrane associated.

Three possible mechanisms could account for the formation of the high-energy retinoids. (i) An irreversible reaction removes the 11-*cis*-retinoids as they are formed. (ii) Specific binding proteins sequester the 11-*cis*-retinoids. (iii) An energy-transducing isomerization reaction uses a membrane constituent as the thermodynamic energy source. We now show that only the last alternative can account for the experimental results, and we provide a mechanism for this process.

We investigated whether the membranes act catalytically in the isomerization reaction or have a limited capacity to form 11-*cis*-retinoids. A membrane preparation was incubated with saturating all-*trans*-retinol until no further 11-*cis*-retinoid accumulated. A control membrane preparation was incubated in the absence of all-*trans*-retinol. The two samples were then briefly irradiated with ultraviolet (UV) light and washed with solutions containing bovine serum albumin (BSA) to remove the remaining retinoids. The UV illumination back isomerizes and eliminates the 11-*cis*-retinoids without di-

Table 1. The esterification-deesterification reactions are reversible. Amphibian (*3*) or bovine (*11*) pigment epithelial membranes (1 ml at a protein concentration of 2 to 3 mg/ml) were incubated with [11, 12-^{3}H]all-*trans*-retinol (Amersham) or its 11-*cis* congener (0.01 mCi at a concentration of 1 μM in 50 μl of 10% BSA) for 15 min at 25°C. The mixtures were then centrifuged at 200,000*g* for 15 min at 4°C, and the pellets were washed and suspended in the original volume of buffer (*3*). Greater than 80% of the radioactivity remained associated with the membranes. One-half of the membrane preparation was removed, and the retinoid composition was analyzed by standard methods (*3*). In the case of the amphibian, the other half of each membrane preparation was incubated for 3 hours at 25°C with 25 μl of 10% BSA and 50 μl of a solution containing NAD^+ and $NADP^+$, each at a concentration of 10 mM, before retinoid analysis. In the bovine case, the membrane preparations were incubated for 1 hour at 37°C with 25 μl of 10% BSA and 50 μl of 10 mM each of NAD^+ and $NADP^+$ for 1 hour at 37°C before analysis of the retinoids. All quoted errors are SEM with n = 3 to 5.

Membrane preparation	Retinoid composition (%)		
	Retinol	Retinal	Retinyl ester
Amphibian			
All-*trans*-retinol	5.3 ± 2.0	4.3 ± 0.4	90.3 ± 2.0
All-*trans*-retinol, NAD^+, and $NADP^+$	5.4 ± 1.7	49.5 ± 4.6	45.0 ± 3.1
Bovine			
All-*trans*-retinol	6.3 ± 2.2	3.9 ± 3.5	89.9 ± 1.3
All-*trans*-retinol, NAD^+, and $NADP^+$	6.0 ± 3.0	49.7 ± 4.1	44.4 ± 7.7
11-*cis*-retinol	12.2 ± 0.0	3.9 ± 0.1	84.0 ± 0.1
11-*cis*-retinol, NAD^+, and $NADP^+$	10.9 ± 0.6	71.1 ± 0.8	17.5 ± 0.1

Department of Biological Chemistry and Molecular Pharmacology, Harvard Medical School, Boston, MA 02115.

---

*To whom correspondence should be addressed.